Hindawi
Mathematical Problems in Engineering
Volume 2021, Article ID 3158504, 8 pages
https://doi.org/10.1155/2021/3158504

Research Article

Analysis of Microscopic Main Controlling Factors for Occurrence of Movable Fluid in Tight Sandstone Gas Reservoirs Based on Improved Grey Correlation Theory

Xuefei Lu,[1] **Fengjuan Dong**,[2,3] **Xiaolong Wei**,[4] **PengTao Wang**,[5] **Na Liu**,[6,7] **and Dazhong Ren**[2,3]

[1]*College of Sciences, Xi'an Shiyou University, Xi'an 710065, Shaanxi, China*
[2]*College of Petroleum Engineering, Xi'an Shiyou University, Xi'an 710065, Shaanxi, China*
[3]*Shaanxi Key Laboratory of Advanced Stimulation Technology for Oil & Gas Reservoirs, Xi'an Shiyou University, Xi'an 710065, Shaanxi, China*
[4]*Changqing Downhole Technology Company, Petro China Chuanqing Drilling Engineering Company Limited, Xi'an 710065, Shaanxi, China*
[5]*Sinopec Green Source Thermal Energy Development Co., Ltd, Xianyang 712000, Shaanxi, China*
[6]*Research Institute of Exploration and Development, Petro China Changqing Oilfield Company, Xi'an 710018, Shaanxi, China*
[7]*National Engineering Laboratory for Exploration and Development of Low Permeability Oil and Gas Fields, Xi'an 710018, Shaanxi, China*

Correspondence should be addressed to Xuefei Lu; luxuefei80@126.com

Received 8 July 2021; Accepted 16 August 2021; Published 21 August 2021

Academic Editor: Feng Xiong

Tight sandstone reservoirs have the characteristics of poor physical properties, fine pore throats, and strong microheterogeneity compared with conventional reservoirs, which results in complicated movable fluid occurrence laws and difficult mining. Taking the tight sandstone gas reservoir of He 8 formation in Sulige gas field as an example, based on physical property test analysis, constant velocity mercury injection, and nuclear magnetic resonance experiments, an optimized gray correlation calculation model is established by improved gray correlation theory, which quantitatively characterizes the influence of microscopic pore structure parameters of different types of tight sandstone gas reservoirs on the occurrence of movable fluids, and the main controlling microgeological factors for the occurrence of movable fluid in tight sandstone gas reservoirs with close/similar physical properties are selected. The results show that the occurrence of movable fluid in Type I reservoirs is mainly affected by the effective pore-throat radius ratio, the saturation of mercury in the total throat, and the effective pore radius, and the occurrence of movable fluid in Type II reservoirs is mainly affected by the effective throat radius per unit volume and total throat mercury saturation and mainstream throat radius. Moreover, the occurrence state of movable fluids in Type II reservoirs is controlled by the throat radius stronger than that of Type I reservoirs. It has important guiding significance for the efficient development of tight sandstone gas reservoirs.

1. Introduction

The exploration and development of tight sandstone oil and gas in unconventional oil and gas occupy an increasingly important position in the field of oil and gas exploration in China [1–3]. Under the coupling action of time, temperature, pressure, and other factors, the creep characteristics of rock particles at different buried depths are different, resulting in different types of reservoirs with different pore structure characteristics, storage and seepage capabilities [4–7]. Pores and throats are the main channels for controlling fluid seepage [8, 9]. The size and distribution of pores and throats affect the connectivity and seepage capacity of pores and throats [10, 11]. A large number of

studies have shown that the proportion set of movable fluids includes reservoir, storage capacity, and fluid storage characteristics, and it is more ideal to characterize the physical properties of ultra-low permeability reservoirs. However, the tight sandstone reservoirs have the characteristics of poor physical properties, small pore throats, and strong microheterogeneity [12–15] compared with conventional reservoirs, which leads to complex reservoirs of movable fluids and difficult mining. At present, new technologies and methodologies are introduced by many scholars to discuss the occurrence of movable fluids in tight reservoirs and their main controlling factors and have achieved certain results. For example, some scholars combine high-pressure mercury intrusion, nitrogen adsorption, image analysis, and other technical methods with nuclear magnetic resonance experiments to reveal the influence of microgeological factors on the occurrence of movable fluids in the reservoir. Studies have shown that the recoverability of oil and gas reservoirs is mainly affected by the pore structure and the occurrence characteristics of movable fluids; the microscopic pore structure characteristics have a significant impact on movable fluids [16–19].

However, their research mainly uses qualitative analysis methods to describe the impact of reservoir microgeological factors on the occurrence of movable fluids. The interaction between various factors has not been considered, and it is difficult to accurately quantify the impact of microgeological factors on the reservoir movable fluids, which has become one of the technical bottlenecks restricting the development of tight oil and gas reservoirs. Therefore, taking the tight sandstone reservoir of He8 formation in Sulige gas field as an example, based on the physical properties of the reservoir, constant velocity mercury intrusion, and nuclear magnetic resonance experiments, the scientific determination resolution coefficient is introduced, and the improved gray correlation analysis model is established to determine the main controlling factors affecting the occurrence of movable fluids in tight sandstone gas reservoirs with near/similar physical properties. It provides reliable microscopic geological basis for finding the "sweet spot" of tight sandstone reservoir and its further efficient development.

2. Experiments and Methods

2.1. Experiments

2.1.1. Experimental Samples and Test Methods

(1) Before Testing, Wash the Sample With Oil. The sample was washed with methanol and dichloromethane mixture in the Soxhlet extracter. When the fluorescence of the washing fluid was very low and unchanged, the washing oil was considered to be finished, and the sample was dried continuously by microwave at 100°C for 24 h.

(2) Porosity-Permeability Test. The experimental methods were strictly carried out in accordance with SY/T6385-1999 "Test method for porosity and permeability of overburden rocks" [20]. FYKS-1 porosity-permeability tester with high temperature and overburden pressure has tested the porosity and permeability. The main technical parameters are as follow: The effective pressure of simulated formation is less than 70 MPa; the effective temperature of simulated formation is less than 150°C; applicable core is $\Phi 25 \times 25 \sim 80$ mm or $\Phi 38 \times 40 \sim 80$ mm; measuring range of permeability is $(0.01 \sim 8000) \times 10^{-3}\ \mu m^2$, measuring range of porosity is less than 50%; measurement precision of permeability is less than 10% for low permeability reservoir and 5% for medium and high permeability reservoir; measurement precision of porosity is 0.5%.

(3) NMR Experiment. The nuclear magnetic resonance T_2 spectrum was measured by MicroMR20-025 from Newmai Company. The main frequency intensity was 23 MHz, the core diameter was 25 mm, the length was 2–4 cm, the echo interval was 0.2 ms, the waiting time was 6 s, and the echo number was 8000. The experimental method is strictly in accordance with SY/T6490-2014 "Laboratory measurement specification for nuclear magnetic resonance parameters of rock samples" [21]. The experiment was carried out at 22°C.

(4) CVMI Experiment. The experimental method was strictly carried out in accordance with GB/T29171-2012 "Rock capillary pressure measurement" [22]. The maximum mercury injection pressure in the constant rate mercury injection test was 0.006895 MPa.

(5) Scanning Electron Microscope. The experimental method was strictly carried out in accordance with SY/T 5162-2014 "Analytical method of rock sample by scanning electron microscope" [23].

(6) Casting Sheet Observation. The experimental methods were strictly carried out in accordance with SY/T 5913-2004 "Rock thin section preparation" [24].

2.2. Dimensionless Method. It is necessary to standardize each parameter [25] for making the parameters comparable, due to the different dimensions of different parameters and the large difference in value. The method is as follows:

(1) For the parameters (excluding parameters other than the effective pore-throat radius ratio) which are positively correlated with reservoir microscopic pore-throat structure characteristics and movable fluid saturation, divide directly by their maximum value.

(2) For parameters that are negatively related to characteristic parameters of reservoir microscopic pore throat structure and saturation of movable fluid (effective pore-throat radius ratio), the maximum value is used to subtract the difference of the parameters and then divided by the maximum value.

2.3. Improved Grey Relevance Theory. The concept of relevance analysis is proposed by Grey system theory, which can provide mathematical analysis methods to clarify the relationship between various factors in the system and find the

most influential factors [26–28]. In the traditional gray correlation analysis method, the resolution coefficient is not quantified but a fixed value 0.5, without considering the distortion of the correlation degree measurement caused by the abnormal value in the data. The improved gray correlation analysis method introduces the quantization process of the resolution coefficient, which makes the calculation process more reasonable [29–31]. The steps are as follows:

The absolute value of reference sequence and the reference sequence subtraction at each point is

$$\Delta_{0i}(k) = \left|X_0(k) - X_i(1)\right|. \tag{1}$$

Maximum range is

$$\Delta_{\max} = \max_i \max_k = \left|X_0(k) - X_i(k)\right|. \tag{2}$$

Minimum range is

$$\Delta_{\min} = \max_i \max_k = \left|X_0(k) - X_i(k)\right|. \tag{3}$$

Correlation coefficient is

$$\varepsilon_{0i}(k) = \frac{\Delta_{\min} + \rho\Delta_{\max}}{\left|\mathbf{X}_0(\mathbf{k}) - \mathbf{X}_i(\mathbf{k})\right| + \rho\Delta_{\max}}, \tag{4}$$

where $\varepsilon_{0i}(k)$ is the relative difference between the comparison curve $X_i(k)$ and the reference curve $X_0(k)$ at time i, which is called the correlation coefficient of $X_i(k)$ to $X_0(k)$ at time i. In order to weaken the influence of the correlation coefficient distortion caused by too large size and enhance the significant difference between correlation coefficients, a coefficient or resolution is artificially introduced, and its value is between 0~1. The quantization method is as follows:

$$\nabla_{ij} = \left|X_0(j) - X_i(j)\right|, \quad (i = 1, 2, \ldots, m;\ j = 1, 2, \ldots, n). \tag{5}$$

Assuming that ∇_θ is the average value of the absolute difference of indicators, then

$$\nabla_\theta = \left(\frac{1}{m}\right)\sum \nabla_{ij}, \quad (i = 1, 2, \ldots, m;\ j = 1, 2, \ldots, n). \tag{6}$$

Let $\varepsilon = \nabla_\theta/\nabla_{\max}$, where $\nabla_{\max} = (\max \nabla_{ij})$.

The value of ρ follows the following principles:

If $1/\varepsilon > 3$, that is, abnormal value, $\varepsilon \le \rho \le 1.5\varepsilon$, let $\rho = 1.5\varepsilon$.

If $2 \le 1/\varepsilon \le 3$ that is, the normal value, $1.5\varepsilon \le \rho \le 2\varepsilon$, let $\rho = 2\varepsilon$.

If $0 < 1/\varepsilon < 2$ that is, the normal value, $2\rho > 1$, let $\rho \in (0.8, 1)$, and 1 is used in this paper.

3. Analysis of Microcontrolling Geological Factors of Movable Fluid Occurrence

3.1. Reservoir Physical Properties and Movable Fluid. Porosity and permeability are not only indicators to characterize reservoir quality, but also closely related to the difficulty and effectiveness of oil and gas field exploitation [19]. It is show that, porosity is distributed in the range of 6.9%~18.3%, with an average of 11.735%; permeability is distributed in the range of $0.065 \times 10^{-3}\,\mu\text{m}^2$ ~$0.747 \times 10^{-3}\,\mu\text{m}^2$, with an average value of $0.291 \times 10^{-3}\,\mu\text{m}^2$, by physical testing and analysis of 10 representative cores in the reservoir of the He 8th member of the study area, and it belongs to a typical tight sandstone gas reservoir. Reservoir porosity has a positive linear correlation with permeability (Figure 1), but the correlation is not strong ($R^2 = 0.488$), which shows that the pore structure of the reservoir is complex, and the physical properties of the reservoir and the fluid flow capacity are controlled by a variety of microgeological factors.

It is found that the movable fluid saturation of the He 8th member in the study area is between 5.38%~32.67%, with an average of 17.56% (Table 1), which based on some scholars' research on the movable fluid of He 8 formation in the east of Sulige gas field.

We have the conclusion that there is a different degree of overlap in information for a single characteristic parameter, by in-depth analysis of the constant velocity mercury intrusion and physical property analysis results of 10 core samples from He 8 reservoir. Therefore, the reservoir quality factor is introduced, denoted by RQI = $\sqrt{K/\phi}$ [19], and it divides the reservoir into two types: I (RQI $\ge$ 0.15) and II (RQI < 0.15) (Table 1).

3.2. Microscopic Pore Structure Characteristics of Reservoir. According to the analysis of casting thin sections and scanning electron microscope data (Figure 2), it can be seen that the reservoir space types of tight sandstone reservoir in He 8 in the study area only include residual intergranular pores, dissolution pores, and intercrystalline pores. It is shown that the pores of the tight sandstone reservoirs in He 8 formation of the study area are macropores, and the pore size and distribution interval are similar, the main pore radius distribution interval is between 120 μm~150 μm and most of the throats belong to the fine throat-thin throat, and the pore throat radius is relatively large (Table 2), based on previous research and analysis of Wang Daofu's pore classification standard and Li Daopin's throat classification standard. The pore-throat configuration relationship of different types of reservoirs is analyzed by mercury margin, which can be denoted by β, and the calculation formula of mercury ingress margin is

$$\beta = \frac{S_t - S_p}{0.01S^2}, \tag{7}$$

where S_t (%) is throat Saturation of Mercury, S_p (%) is pore mercury saturation, and S (%) is total mercury saturation.

It is found that the mercury ingress margin for type I reservoirs is 0.24~1.47, the average value is 0.837; the mercury ingress margin of type II reservoirs is 2.09~3.7, and the average value is 2.958; the percentage of mercury ingress in the throat of type I and II reservoirs is gradually increasing, and the reservoir is gradually controlled by the throat, based on the constant velocity mercury intrusion experiment results of 10 rock samples from the He 8th reservoir in the study area and using formula (1) to calculate the mercury ingress margin of each sample. At the same

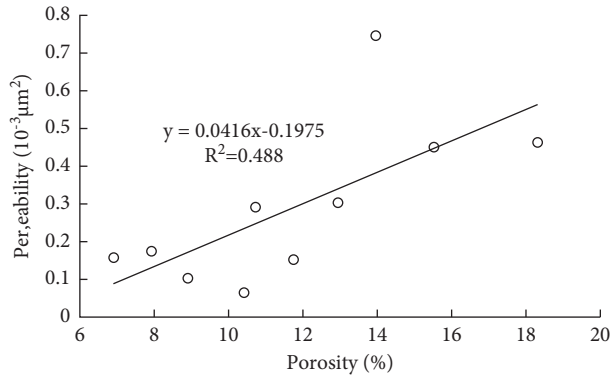

Figure 1: Relationship between porosity and permeability of He 8 tight sandstone reservoir.

Table 1: Laboratory results of samples in the east of Sulige gas field with nuclear magnetic resonance technique [16].

Sample no	Φ/(%)	$K/(10^{-3}\,\mu m^2)$	RQI	S_m/(%)	Type
1#	13.96	0.747	0.23	26.35	I
2#	18.30	0.463	0.16	13.78	I
3#	10.41	0.065	0.08	5.38	II
4#	15.52	0.45	0.17	32.67	I
5#	8.89	0.104	0.11	8.48	II
6#	12.95	0.304	0.15	21.88	I
7#	10.74	0.291	0.16	26.05	I
8#	6.90	0.157	0.15	17.39	I
9#	7.93	0.174	0.14	15.62	II
10#	11.75	0.154	0.11	8.02	II

time, the analysis of the relationship between each microscopic pore structure characteristic parameter and movable fluid saturation found (Figure 3) showed that only mercury intake margin and effective pore throat radius ratio were negatively correlated with movable fluid saturation, while other parameters were positively correlated with movable fluid saturation, and the correlation was significantly different.

3.3. Grey Correlation Degree between Micropore Structure Characteristic Parameters and Movable Fluid Saturation. The movable fluid and micropore characteristic parameters of 10 samples from the He 8 tight sandstone reservoir in Sulige Gas Field were selected as the research object (Tables 1 and 2), Based on the results of reservoir classification, the same type of reservoir is used and the improved grey correlation theory is selected to quantitatively characterize the influence of the microscopic pore structure characteristic parameters of near/similar reservoirs on the occurrence of movable fluids.

According to the relevant data of each parameter in Tables 1 and 2, the movable fluid saturation and the characteristic parameters of the micropore are regarded as the parent sequence and the subsequence, respectively Taking the improved gray correlation theory, determine the gray correlation degree ranking between the microscopic pore structure characteristic parameters of the near/similar reservoirs and the movable fluid saturation, as shown in Table 3.

It can be seen from Table 3 that the relationship between the characteristic parameters of microscopic pore throats and the movable fluid saturation and their rankings show that the movable fluid saturation of Type I reservoirs is mainly affected by the effective pore-throat radius ratio, the total throat mercury saturation, and the effective pores radius. These three characteristic parameters reflect the pores, throat size, and pore-throat configuration relationship and determine the effective way of fluid passage and the degree of restraint in the pores, indicating that the existence law of movable fluid in this type of reservoir is restricted by the connection of effective pore throats. Movable fluid saturation in Type II reservoirs is mainly affected by three factors:

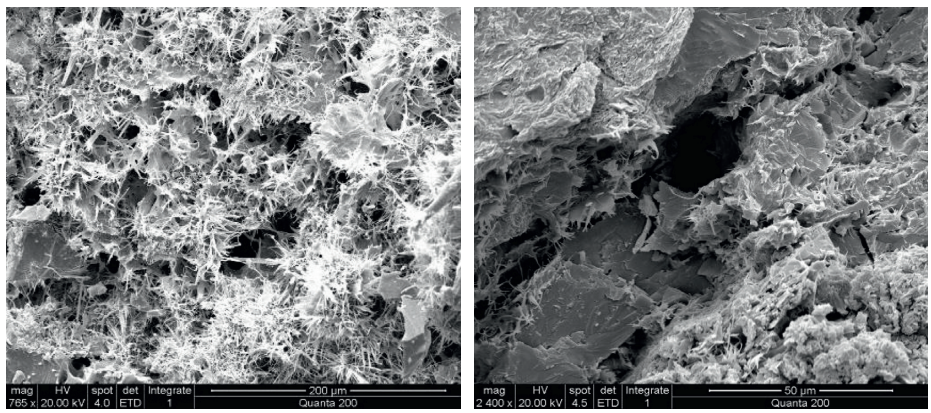

5#, 3137.23 m
Illite intercrystalline pore

1#, 2747.85 m
Residual intergranular pore

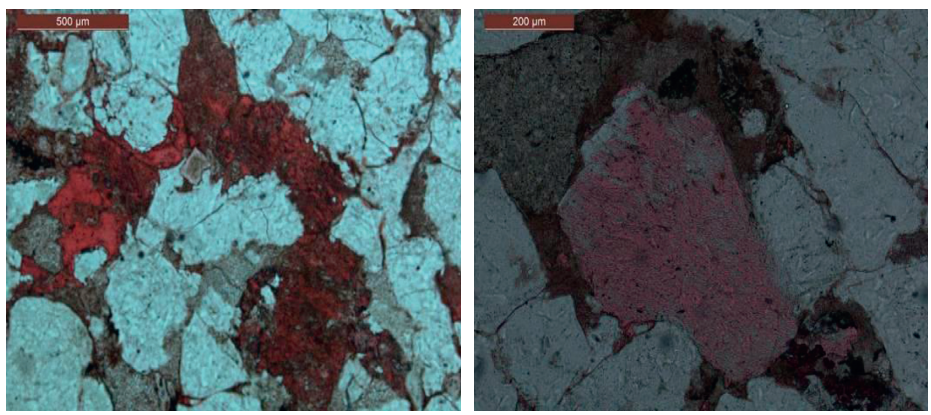

4#, 3137.23 m, 12/5000
Dissolved pores and residual filamentous clay minerals

7#, 2627.66 m
Feldspar dissolved pore

Figure 2: The reservoir space types of tight sandstone reservoir in He 8 in the study area.

Table 2: Pore structure parameters of the He 8 reservoir in the east of Sulige gas field [16].

Sample no	Total pore mercury saturation (%)	Mercury saturation total throat	Effective pore radius (μm)	Effective throat radius (μm)	Main flow throat radius (μm)	Effective throat volume (puv) ml/cm^3	Effective pore volume (puv) m^3	Effective pore throat radius ratio	Sorting coefficient	Mercury margin	Type
1#	15.48	35.36	153.31	0.910	0.881	0.017	0.037	227.5	0.26	0.77	I
2#	12.46	23.80	152.57	0.689	0.636	0.043	0.027	235.5	0.21	0.86	I
3#	2.44	18.17	118.04	0.544	0.665	0.019	0.002	563.2	0.10	3.70	II
4#	24.88	32.99	149.23	0.982	1.126	0.051	0.031	214.6	0.36	0.24	I
5#	5.76	13.50	143.99	0.656	0.487	0.012	0.013	432.5	0.20	2.09	II
6#	19.31	32.86	144.28	0.645	0.733	0.043	0.025	227.5	0.24	0.50	I
7#	10.57	33.69	143.99	0.704	0.815	0.017	0.036	263.5	0.19	1.18	I
8#	8.48	24.82	136.40	0.743	0.613	0.019	0.014	194.6	0.16	1.47	I
9#	2.88	25.48	116.73	0.620	0.632	0.009	0.021	241.7	0.21	2.81	II
10#	0.79	28.48	129.15	0.643	0.314	0.031	0.016	352.8	0.07	3.23	II

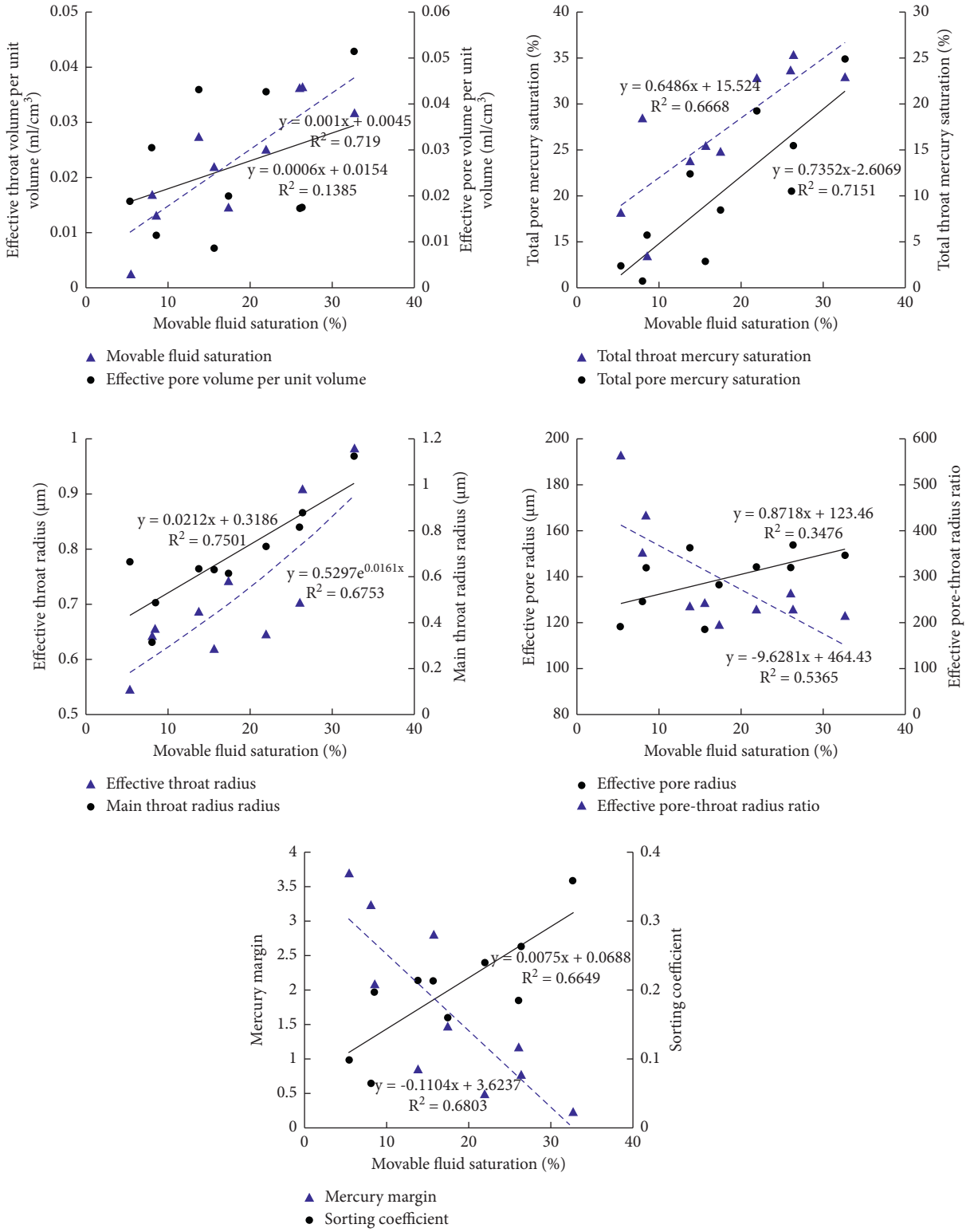

Figure 3: Relationship between micro pore structure characteristic parameters and movable fluid saturation.

Table 3: Correlation degree and ranking of microscopic pore-throat characteristic parameters and movable fluid saturation.

	Effective pore throat radius ratio weighted average	Mercury saturation of total throat	Weighted average of effective pore radius	Effective pore volume per unit volume	Effective throat radius weighted average	Total pore mercury saturation	Main flow throat radius	Effective throat volume per unit volume	Sorting coefficient	Reservoir types of
Correlation	0.806	0.756	0.735	0.731	0.723	0.708	0.695	0.673	0.455	I reservoir
Ranking	1	2	3	4	5	6	7	8	9	
Correlation	0.792	0.803	0.796	0.711	0.674	0.712	0.802	0.810	0.715	II
Ranking	5	2	4	8	9	7	3	1	6	reservoir

effective throat volume per unit volume, total throat mercury saturation, and mainstream throat radius. We can get the conclusion that the presence of fluid in the effective throat of this type of reservoir has absolute control over the distribution of movable fluid.

4. Results and Conclusions

(1) The average value of pores in He 8 tight sandstone reservoir of the study area is 11.735%, and the average of permeability is $0.291\times10^{-3}\,\mu m^2$, which is a typical tight sandstone reservoir. Taking the size of the reservoir quality factor as the evaluation criterion, the reservoir is divided into two types, I and II, and the quality of the reservoir gradually deteriorates, and the physical properties of similar reservoirs are similar.

(2) Using different types of reservoirs as data sets, the improved grey correlation theory was used to quantitatively characterize the influence of the microscopic pore structure of reservoirs with near/similar physical properties on the occurrence of movable fluids. Among them, the movable fluid saturation of Type I reservoirs is mainly affected by the effective pore-throat radius ratio, the total throat saturation of mercury, and the effective pore radius. The movable fluid saturation of Type II reservoirs is mainly affected by the effective throat volume per unit volume, the influence of the mercury saturation of the total throat and the radius of the mainstream throat. Therefore, the occurrence state of movable fluids in Type II reservoirs is controlled by the throat radius stronger than in Type I reservoirs.

(3) It is shown that the reservoirs in He 8 tight sandstone reservoir of the study area are mainly of throat type, and the mercury ingress margin of type I reservoirs is significantly less than that of type II reservoirs; the proportion of mercury in the throats of type I and II reservoirs is gradually increasing, and the reservoirs are affected by throats. The control effect is gradually increasing. Based on the constant velocity mercury injection experiment, the "mercury ingress margin" was introduced to analyze the pore-throat configuration relationship of different types of reservoirs in He 8 tight sandstone reservoir of the study area.

Data Availability

The data used to support the results of this study are included within the manuscript.

Conflicts of Interest

The authors declare that there are no conflicts of interest.

Acknowledgments

This work was financially supported by the National Natural Science Foundation of China (41802166 and 51934005), Shaanxi Provincial Key Research and Development Program (2021GY-140), Opening Foundation of Shaanxi Key Laboratory of Advanced Stimulation Technology for Oil & Gas Reservoirs (20JS120), Open Foundation of Key Laboratory of Coal Resources Exploration and Comprehensive Utilization, Ministry of Natural Resources (KF2021-3), and Shaanxi Provincial Key Research and Development Program (2021GY-140).

References

[1] J. H. Fu, J. Yu, and L. M. Xu, "New progress in exploration and development of tight oil in ordos basin and main controlling factors of large-scale enrichment and exploitable capacity," *China Petroleum Exploration*, vol. 20, no. 5, pp. 9–19, 2015.

[2] H. Yang, S. X. Li, and X. Y. Liu, "Characteristics and resource prospects of tight oil and shale oil in ordos basin," *Acta Petrolei Sinica*, vol. 34, no. 1, pp. 1–11, 2013.

[3] C. N. Zou, *Unconventional Petroleum Geology*, Geological Publishing House, Beijing, China, 2011.

[4] C. Zhu, M. He, M. Karakus, X. Zhang, and Z. Tao, "Numerical simulations of the failure process of anaclinal slope physical model and control mechanism of negative poisson's ratio cable," *Bulletin of Engineering Geology and the Environment*, vol. 80, no. 4, pp. 3365–3380, 2021.

[5] Y. Wang, W. K. Feng, R. L. Hu, and C. H. Li, "Fracture evolution and energy characteristics during marble failure under triaxial fatigue cyclic and confining pressure unloading (FC-CPU) conditions," *Rock Mechanics and Rock Engineering*, vol. 54, no. 2, pp. 799–818, 2021.

[6] F. Wu, H. Zhang, Q. L. Zou et al., "Viscoelastic-plastic damage creep model for salt rock based on fractional derivative theory," *Mechanics of Materials*, vol. 150, Article ID 103600, 2020.

[7] Q. Yin, J. Wu, C. Zhu et al., "Shear mechanical responses of sandstone exposed to high temperature under constant normal stiffness boundary conditions," *Geomechanics and Geophysics for Geo-Energy and Geo-Resources*, vol. 7, no. 2, p. 35, 2021.

[8] E. Aliakbardoust and H. Rahimpour-Bonab, "Effects of pore geometry and rock properties on water saturation of a carbonate reservoir," *Journal of Petroleum Science and Engineering*, vol. 112, pp. 296–309, 2013.

[9] Y. J. Gong, S. B. Liu, M. J. Zhao, H. B. Xie, and K. Y. Liu, "Characterization of micro pore throat radius distribution in tight oil reservoirs by NMR and high pressure mercury injection," *Petroleum Geology & Experiment*, vol. 38, no. 3, pp. 389–394, 2016.

[10] G. Desbois, J. L. Urai, P. A. Kukla, J. Konstanty, and C. Baerle, "High-resolution 3D fabric and porosity model in a tight gas sandstone reservoir: a new approach to investigate microstructures from mm to nm-scale combining argon beam cross-sectioning and SEM imaging," *Journal of Petroleum Science and Engineering*, vol. 78, no. 2, pp. 243–257, 2011.

[11] N. Liu, Z. H. Zhou, D. Z. Ren et al., "Distribution characteristics and controlling factors of movable fluid in tight sandstone gas reservoir: a case study of the eighth member of xiashihezi formation and the first member of Shanxi formation in western sulige gas field," *Lithologic Reservoirs*, vol. 31, no. 6, pp. 14–25, 2019.

[12] G. Wang, X. Chang, W. Yin, Y. Li, and T. Song, "Impact of diagenesis on reservoir quality and heterogeneity of the upper triassic chang 8 tight oil sandstones in the Zhenjing area, ordos basin, China," *Marine and Petroleum Geology*, vol. 83, pp. 84–96, 2017.

[13] A. Sakhaee-Pour, "Decomposing J-function to account for the pore structure effect in tight gas sandstones," *Transport in Porous Media*, vol. 116, no. 2, pp. 453–471, 2017.

[14] B. Bai, R. K. Zhu, S. T. Wu et al., "Multi-scale method of nano (micro)-CT study on microscopic pore structure of tight sandstone of Yanchang formation, ordos basin," *Petroleum Exploration and Development*, vol. 40, no. 3, pp. 329–333, 2013.

[15] D. K. Liu, W. Sun, D. Z. Ren et al., "Feature of pore-throat structures and movable fluid in tight gas reservoir: a case from He 8 formation of permian xiashihezi Formation and the 1st member of permian Shanxi formation in the western area of sulige gas field, ordos basin," *Natural Gas Geoscience*, vol. 27, no. 12, pp. 2136–2145, 2016.

[16] D. Z. Ren, W. Sun, T. Lu et al., "Microscopic geological factors of movable fluid distribution in the tight sandstone gas reservoir: taking the He 8 reservoir in the east of sulige gas field as an example," *Geoscience*, vol. 6, no. 29, pp. 1409–1417, 2015.

[17] Y. Ren, W. Sun, X. Zhang et al., "Characteristics of movable fluids and study of production performance in different flow units of low-permeability reservoir: an example from the chang 6 block of the jiyuan oilfield in ordos basin," *Geology and Exploration*, vol. 52, no. 5, pp. 974–984, 2016.

[18] H. X. Ming, W. Sun, L. L. Zhang, and Q. Wang, "Impact of pore structure on physical property and occurrence characteristics of moving fluid of tight sandstone reservoir: taking He 8 reservoir in the east and southeast of sulige gas field as an example," *Journal of Central South University (Science and Technology)*, vol. 46, no. 12, pp. 4556–4567, 2015.

[19] D. Z. Ren, W. Sun, F. J. Dong, H. Hang, and X. F. Qu, "Characteristics of movable fluids in the chang 81 reservoir, yanchang formation in huaqing oilfield, ordos basin and the influencing factors," *Geology and Exploration*, vol. 51, no. 4, pp. 797–804, 2015.

[20] State Bureau of Petroleum and Chemical Industry, *The Porosity and Permeability Measurement of Core in Net Confining Stress: SY/T6385-1999*, Petroleum Industry Press, Beijing, China, 1999.

[21] National energy administration, *Standard for Laboratory Measurement of NMR Parameters of Rock Samples: SY/T6490-2014*, Petroleum Industry Press, Beijing, China, 2015.

[22] Standardization Administration of China, *Rock Capillary Pressure Measurement: GB/T29171-2012*, Petroleum Industry Press, Beijing, China, 2012.

[23] National Energy Administration, *Analytical Method of Rock Sample by Scanning Electron Microscope: SY/T 5162-2014*, Petroleum Industry Press, Beijing, China, 2014.

[24] National development and reform commission, *Rock Thin Section Preparation: SY/T 5913-2004"*, Petroleum Industry Press, Beijing, China, 2004.

[25] F. J. Dong, X. F. Lu, and Y. P. Ma, "Comprehensive evaluation of methane reservoirs based on TOPSIS," *Geology and Exploration*, vol. 51, no. 3, pp. 587–591, 2015.

[26] X. F. Lu, F. J. Dong, X. S. Bo, Y. Cao, and H. Huang, "Quantitative characterization of the effect of micro pore structure on reservoir quality of tight sandstone reservoirs based on improved grey correlation theory," *Mathematics in Practice and Theory*, vol. 51, no. 4, pp. 99–108, 2021.

[27] F. J. Dong, X. F. Lu, M. Y. Liu, and X. J. Rao, "Correlation analysis of microscopic geological factors and micro cracks based on the grey association," *Geology and Exploration*, vol. 52, no. 5, pp. 950–955, 2016.

[28] S. Y. Xie, Y. Wang, Y. B. Xie, and H. B. Li, "Application of grey system theory to determining order of ICA decrypted images," *Journal of Northwestern Polytechnical University*, vol. 33, no. 1, pp. 153–158, 2015.

[29] Z. Q. Zhang, B. Q. Hu, Y. Li, and J. H. Wei, "Study of growth poles and factors driving land consolidation in guangxi based on improved grey relational analysis method," *Journal of Agricultural Resources and Environment*, vol. 36, no. 4, pp. 431–440, 2019.

[30] Y. B. Dong and Z. S. Duan, "New determination method for identification coefficient of grey relational grade," *Journal of Xi'an University of Architecture & Technology*, vol. 40, pp. 589–592, 2008.

[31] X. F. Lu, X. Y. Wang, Y. F. Yang, and J. N. Xue, "The optimization model for reducing RON loss in gasoline refining process," *Geofluids*, vol. 2021, Article ID 5520942, 10 pages, 2021.